PROTEIN STRUCTURE REPORT

Non-3D domain swapped crystal structure of truncated zebrafish alphaA crystallin

A. Laganowsky[1,2,3] and D. Eisenberg[1,2,3]*

[1]UCLA-DOE, Institute for Genomics and Proteomics, Los Angeles, California
[2]Department of Chemistry and Biochemistry, University of California Los Angeles, Los Angeles, California
[3]Howard Hughes Medical Institute

Received 21 May 2010; Revised 5 July 2010; Accepted 6 July 2010
DOI: 10.1002/pro.471
Published online 28 July 2010 proteinscience.org

Abstract: In previous work on truncated alpha crystallins (Laganowsky et al., Protein Sci 2010; 19:1031–1043), we determined crystal structures of the alpha crystallin core, a seven beta-stranded immunoglobulin-like domain, with its conserved C-terminal extension. These extensions swap into neighboring cores forming oligomeric assemblies. The extension is palindromic in sequence, binding in either of two directions. Here, we report the crystal structure of a truncated alphaA crystallin (AAC) from zebrafish (*Danio rerio*) revealing C-terminal extensions in a non three-dimensional (3D) domain swapped, "closed" state. The extension is quasi-palindromic, bound within its own zebrafish core domain, lying in the opposite direction to that of bovine AAC, which is bound within an adjacent core domain (Laganowsky et al., Protein Sci 2010; 19:1031–1043). Our findings establish that the C-terminal extension of alpha crystallin proteins can be either 3D domain swapped or non-3D domain swapped. This duality provides another molecular mechanism for alpha crystallin proteins to maintain the polydispersity that is crucial for eye lens transparency.

Keywords: X-ray diffraction; small heat shock protein; protein chaperone; cataract; eye lens transparency; alpha crystallin

Abbreviations: 3D, three-dimensional; AAC, alphaA crystalline; ABC, alphaB crystalline; AP, antiparallel beta sheet interface; APx, antiparallel beta sheet interface registration state x; $bAAC_{59–163}$, bovine alphaA crystallin residues 59–163; $bAAC_{59–163}$-Zn, zinc bound form of bovine alphaA crystallin residues 59–163; $hABC_{68–162}$, human alphaB crystallin residues 68–162; Hsp, heat shock protein; zfAAC, zebrafish alphaA crystalline; $zfAAC_{60–166}$, zebrafish alphaA crystalline.

Additional Supporting Information may be found in the online version of this article.

Grant sponsor: NIH Chemistry Biology Interface Training Program; Grant number: 5T32GM008496; Grant sponsor: DOE BER; Grant number: DE-FC02-02ER63421; Grant sponsor: NIH National Center for Research Resources; Grant number: RR-15301; Grant sponsor: DOE; Grant number: DE-AC02-06CH11357.

**Correspondence to:* D. Eisenberg, Howard Hughes Medical Institute, UCLA-DOE Institute for Genomics and Proteomics, Los Angeles, CA 90095-1570. E-mail: david@mbi.ucla.edu

Introduction

Alpha crystallins are eye lens proteins functioning in light refraction and in maintaining lens transparency. In zebrafish (*Danio rerio*), the alpha crystallins comprise 7–22% of eye lens proteins depending on the age of the fish,[1–3] a lower percentage than the up to 50% reached in some mammalian lenses.[4] Although the percentage of alpha crystallin is lower in zebrafish, the ratio of alphaA crystallin (AAC) to alphaB crystallin (ABC) is roughly 3:1 for zebrafish, similar to human.[2,5] In function, zebrafish AAC (zfAAC) expression has been shown to rescue gamma crystallin protein insolubility in the zebrafish *cloche* mutant, preventing cataract formation.[6] This zebrafish *cloche* mutant highlights the importance of AAC in eye lens development.

Recently, both we and Bagneris *et al.*[7] discovered that truncated constructs of alpha crystallins form crystals. This discovery led to two crystal structures of truncated human ABC: one of the alpha crystallin core domain, residues 67–157,[7] and the other, residues 68–162 ($hABC_{68–162}$),[1] containing the conserved C-terminal extension. Also, there are two crystal structures for a truncated bovine AAC, residues 59–163 ($bAAC_{59–163}$),[1] containing the C-terminal extension.

From our previous work,[1] we found that alpha crystallins encode polydispersity that supports eye lens transparency and chaperone function. A dimeric interface is formed by an antiparallel beta sheet,[1,7–11] called the AP interface.[1] This AP interface appears dynamic with three distinct registration states. The three registration states have been defined according to their degree of surface area buried as AP_I, AP_{II}, and AP_{III},[1,7] with AP_I registration state having the greatest surface area buried. The C-terminal extension can structurally be divided into two sections; hinge loop and tail.[1] The hinge loop forms a flexible loop that allows binding to neighboring molecules. For example, in one of the $bAAC_{59–163}$ structures, the hinge loop is disordered, and in the second, the hinge loop is ordered, positioning a key histidine residue involved in a Zinc-binding motif ($bAAC_{59–163}$-Zn).[1] The C-terminal tail contains a conserved palindromic sequence motif that allows for bidirectional binding.[1] Taken together, all of these features enforce polydisperse and short-range interactions within the alpha crystallins in support of eye lens function.[1,12–15]

Three-dimensional (3D) domain swapping has been observed for alpha crystallin and related proteins. In 3D domain swapping, a protein domain breaks its noncovalent bonds with the core domain and swaps into the same environment in an identical molecule, producing an oligomeric assembly (for review see Refs. 16–20). In crystal structures of truncated alpha crystallins ($bAAC_{59–163}$[1] and $hABC_{68–162}$[1]), the C-terminal extension is 3D domain swapped as in homologous structures (Wheat Hsp16.9[21] and *Methanococcus janaschii* Hsp16.5[22]). In these structures, the C-terminal extension is swapped into adjacent molecules forming run-away oligomeric assemblies. In the case of the homologous structures, Wheat Hsp16.9 and *M. janaschii* Hsp 16.5, the C-terminal extensions 3D domain swap to form oligomeric assemblies.

Other eye lens crystallins also 3D domain swap. Gamma and beta crystallins contain two domains, with each domain containing two Greek key structural motifs, which are joined by a linker (for review see Ref. 23). For example, in the structure of γ-crystallin II monomer,[24] the linker between domains supports non-3D domain swapping to form a closed monomer.[19] For beta crystallin, the amino acid sequence and linker support both 3D domain swapping and non-3D domain swapped closed structures. For example, a 3D domain swapped dimer of βB2-crystallin, with an extended linker, assembles into a tetrameric oligomer.[25,26] βB1-crystallin, with sequence identity of 58% to βB2-crystallin,[26] forms a dimer without 3D domain swapping.[27] Furthermore, a homologous protein of the beta–gamma crystallin family, nitrollin from *Nitrosospira multiformis*, contains a single domain that forms a dimer through 3D domain swapping.[28]

Figure 1. Amino acid sequence alignment of truncated alpha crystallins from zebrafish (*Danio rerio*), antartic cod (*Dissostichus mawsoni*), human (*Homo sapiens*), and bovine (*Bos taurus*). Residue numbers are listed below amino acid sequences. Beta-strand assignments are shown at top of alignment. Identical residues are shaded in gray and similar residues are shaded in light gray.

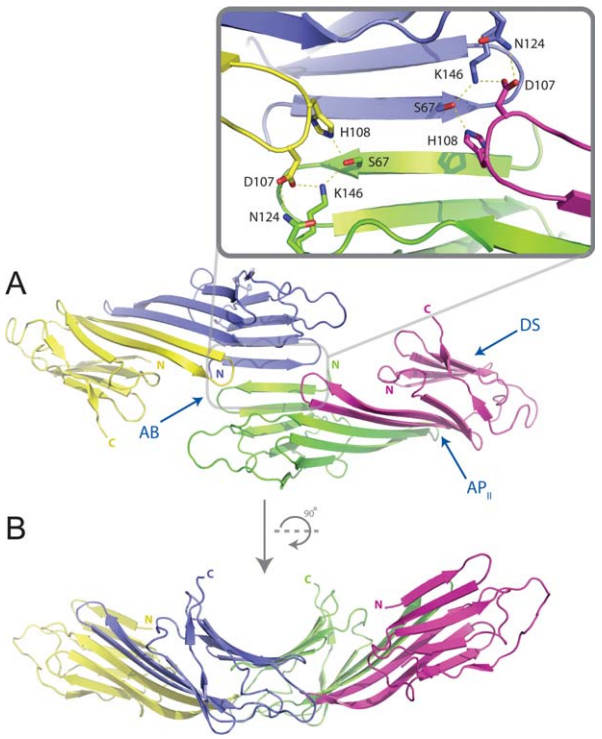

Figure 2. Crystal structure of truncated zebrafish alphaA crystallin (zfAAC$_{60–166}$). Four molecules form a tetramer mediated through a previously unobserved dimeric interface (AB). The asymmetric unit contains two chains that form a dimeric interaction through an interface (AP) common to all vertebrate small heat shock proteins of known structure, with a registration state of AP$_{II}$.[1] Shown are four molecules generated by the twofold symmetry operation on the dimer of the asymmetric unit. N- and C-termini labels are color coded for each chain. A: A total of four chains form the closed tetramer were each C-terminal extension binds to its own domain (DS). The inset is an enlarged view of the dimeric interface, AB, created by beta strand β2 and the loop, located in between strands β5 and β6. Residue numbers are shown. Hydrogen bonds are shown by dashed yellow lines. B: A 90° rotation of the closed tetramer about a horizontal axis.

Here, we present the first structure of a truncated alpha crystallin with C-terminal extension in a non-3D domain swapped, closed state, and present evidence that the closed monomer can transform into a 3D domain swapped dimer.

Results

Our truncated form of zfAAC contains residues 60–166 (zfAAC$_{60–166}$) including the C-terminal quasi-palindromic motif,[1] with amino acid sequence of D**R**T**IPV**T**R**EDK. The truncated amino acid sequence of zfAAC is highly similar to AAC of antartic cod (*Dissostichus mawsoni*) Fig. 1. Both bovine and human AAC show major differences to zfAAC in the hinge loop region Fig. 1.

The structure of zfAAC$_{60–166}$ reveals the first alpha crystallin structure having non-3D domain swapping of the C-terminal extension (Fig. 2 and Table 1). There are two chains located in the asymmetric unit cell of the immunoglobulin-like alpha crystallin core domain of seven beta strands that form a tetrameric assembly. Within this tetrameric assembly, the C-terminal extensions extend from the core domain wrapping around to cap their own domain by binding of the quasi-palindromic C-terminal tail. This non-3D domain swapping of the C-terminal extension is in contrast to the 3D domain swapped

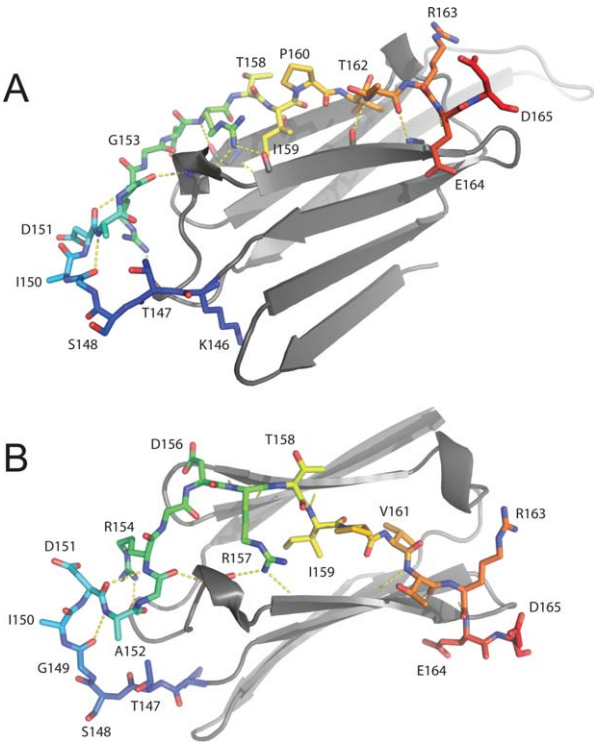

Figure 3. Molecular interactions of the non-3D domain swapped C-terminal extension. The C-terminal extension, residues 146–165, backbone carbon atoms are colored in rainbow with carbonyl oxygen atoms red and nitrogen atoms blue. Remaining residues are shown as a gray ribbon. Hydrogen bonds are shown by dashed yellow lines and residues are labeled. A side view (panel A) and top view (panel B) are shown. Extending from the crystallin domain, the hinge loop forms a beta hairpin structure. R154 and the carbonyl of G153 of the structured hinge loop form hydrogen bonds with the crystallin core domain and position the C-terminal tail. The C-terminal tail binds in the orientation opposite to that in bAAC$_{59–163}$,[1] which is 3D domain swapped. Three backbone hydrogen bonds are made each by residues 157–159 and residues 162–164, located on both sides for the C-terminal tail. Additional hydrogen bonds are made by the side chain of D156 to the amide of D92, the side chain of R154 to the side chain of D93 and carbonyl of S123, and the side chain of R157 to carbonyls of I130 and Q127. Hydrophobic interactions are formed by the burial of I159 and V161 into a hydrophobic groove, created by strands β4 and β8, located on top of the alpha crystallin domain.

Table I. *X-Ray Data Collection and Refinement Statistics for Truncated Zebrafish AlphaA ($zfAAC_{60–166}$) Crystallin*

	$zfAAC_{60–166}$
Crystal parameters	
Space group	$P4_32_12$
Unit cell dimensions (Å)	$a = b = 33.29$, $c = 354.33$
Angles (°)	$\alpha = \beta = \gamma = 90$
Data collection	
Synchrotron (beam line)	APS (24-ID-E)
λ (Å)	0.979
Resolution (Å)	27.82–1.75
R_{fac} (%)[a]	6.3 (34.4)
I/σ	23.7 (4.3)
Reflections observed/unique	148,485/21,407
Completeness (%)	98 (99)
Refinement	
R_{work}(%)	20.5
R_{free} (%)	24.8[b]
Number of protein atoms	1705
Number of water molecules	172
RMSD bond/angle (Å/°)	0.007/1.11
Protein atoms average B-factor ($Å^2$)	24
Ramachandran map, favored/allowed (%)	95/4.6
PDB accession code	3N3E

Values in parentheses correspond to the highest resolution shell.
[a] $R_{fac} = \Sigma |I - \langle I \rangle| / \Sigma I$.
[b] R_{free} calculated using 5% of the data.

C-terminal extensions of $bAAC_{59–163}$ and $hABC_{68–162}$, which are bound to adjacent molecules.

Dimeric interface

A tetrameric assembly is created by two dimeric interfaces. One dimeric interface, termed AP, is created by two identical beta strands on the neighboring molecules (Fig. 2). The registration of the two strands is of the AP_{II}[1] type we observed in $bAAC_{59–163}$. A previously unobserved type of dimeric interface is created through an interaction of edge beta strands, β2 of the alpha crystallin domain, to form the tetrameric assembly. This dimeric interface is further stabilized by residues located in the loop region between β5 and β6 + 7. These loops bend inward toward the β2 beta strands forming hydrogen bonds through residues aspartate 107 and histidine 108 to serine 67, asparagine 124, and lysine 146 [Fig. 2(A), inset].

Non-3D domain swapped C-terminal extension

The C-terminal extension of $zfAAC_{60–166}$ is unique among the alpha crystallins of known structure in that it is non-3D domain swapped. Extending outward the C-terminal extension wraps around to bind to the top of the core domain of the same molecule, which is defined as the closed state[29] (Fig. 3). In contrast, the swapped state refers to the C-terminal extension when 3D domain swapped, for example, in $bAAC_{59–163}$ and $hABC_{68–162}$.[1] Thus, the non-3D domain swapped C-terminal extensions of $zfAAC_{60–166}$ create a tetrameric oligomer.

The structure displays two conformations of the hinge loop. In one conformation, the hinge loop contains two beta hairpin structural motifs that are roughly perpendicular to the beta strands of the alpha crystallin core domain (Fig. 3) with clear electron density (Supporting Information Fig. S1). This beta hairpin motif is reminiscent of the *"w"*-like structure composed of three beta hair-pin structural motifs in $bAAC_{59–163}$[1] (Supporting Information Fig. S2). In a second conformation, the hinge loop forms a large loop. Similar molecular interactions position the hinge loop of $zfAAC_{60–166}$ in these two conformations. In both conformations, the carbonyl hydrogen of hinge loop glycine 153 bonds to the amide of serine 128. The side chain of arginine 154 hydrogen bonds to both the carbonyl of serine 123 and the side chain of aspartate 93 in one of its two conformations and to the side chain of aspartate 93 in its second conformation.

Several molecular interactions stabilize the bound C-terminal quasi-palindromic tail. Residues 156–166 in both chains of $zfAAC_{60–166}$ are similar, with differences for residues 163–166. Two short beta strands, β10 and β11 Fig. 1, are formed on each side of the C-terminal tail (Figs. 3 and 4). For both chains, C-terminal tail side chain of aspartate 156 hydrogen bonds to amide of aspartate 92, and side chain of arginine 157 forms hydrogen bonds to both carbonyl of serine 128 and carbonyl of isoleucine 159. In short, these molecular interactions are similar to other truncated alpha crystallins.

The quasi-palindromic C-terminal tail supports bidirectional binding with pseudo-twofold symmetry. The C-terminal tail is bound to the core domain in the opposite direction of the tail of $bAAC_{59–163}$[1] and in the same direction as the tails of $hABC_{68–162}$,[1] Wheat Hsp16.9,[21] and *M. janaschii* Hsp16.5.[22] Structural comparison of the oppositely bound C-terminal tails of $zfAAC_{60–166}$ and $bAAC_{59–163}$ reveals a pseudo twofold symmetry axis centered on proline 160 (Fig. 4). The flanking palindromic arginines display differing rotamer conformations, while other residues nearly overlay.

3D and Non-3D swapping of the C-terminal extension

The energetic barrier to swapping of the C-terminal extension of AAC is evidently small as shown by the shift in equilibrium toward the 3D domain swapped state from the non-3D domain swapped state that is achieved by heating and subsequent cooling of a solution of $zfAAC_{60–166}$. Native polyacrylamide gel electrophoresis resolves a native dimer, while on heating and subsequent cooling, an additional band of larger molecular weight is observed (Supporting Information Fig. S3). This larger molecular weight

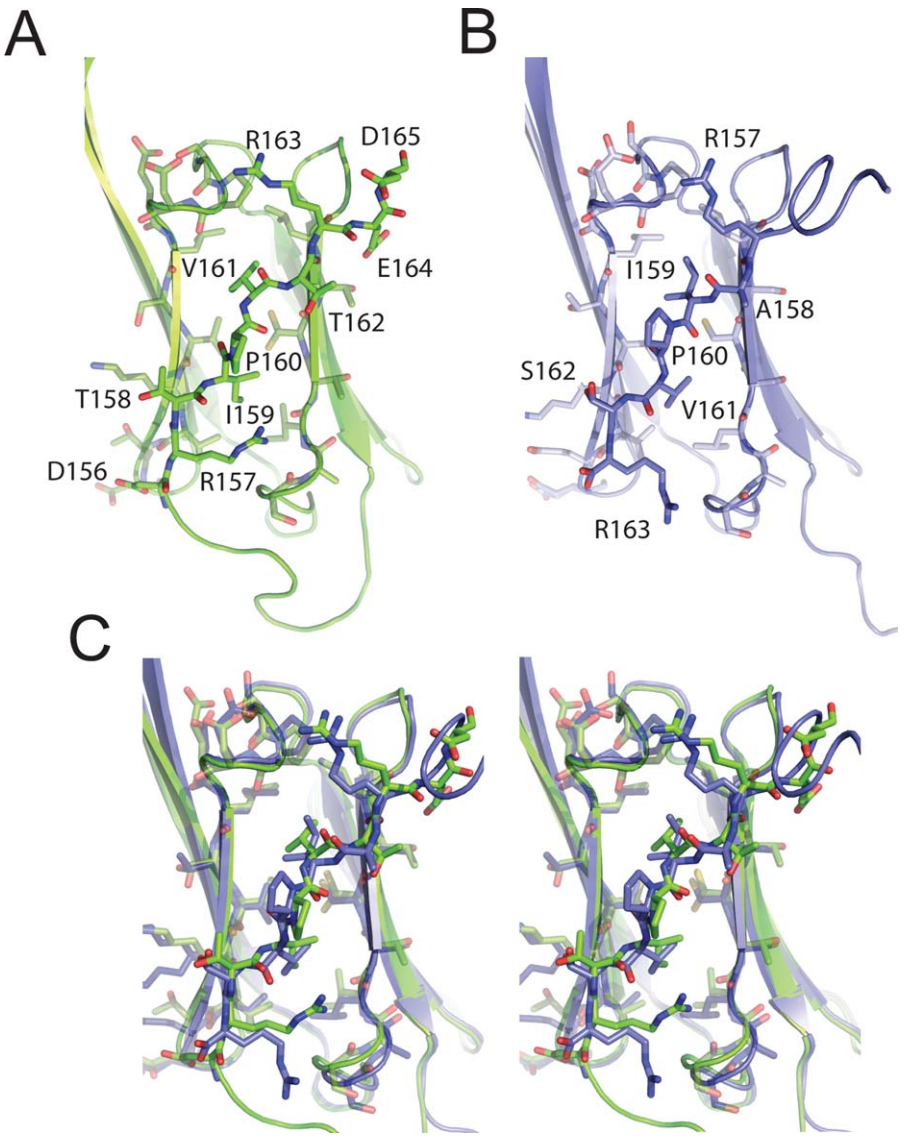

Figure 4. Bidirectional binding of the alphaA crystallin palindromic C-terminal tail. Residues labels are shown in panels A and B. The zfAAC$_{60–166}$ non-3D domain swapped C-terminal tail and interacting residues, located at the top of the crystallin core domain, are shown with carbon atoms colored green and noncarbon atoms colored by atom type (panel A). The 3D domain swapped C-terminal tail of bAAC$_{59–163}$ (pdb 3L1E)[1] is shown with carbon atoms colored in blue and noncarbon atoms colored by atom type. The interacting residues, located at the top of the crystallin core domain, are shown with carbon atoms colored in light blue and noncarbon atoms colored by atom type (panel B). The hinge loop is located on the bottom left and top right for zfAAC$_{60–166}$ and bAAC$_{59–163}$, respectively. The palindromic C-terminal tail allows the C-terminal tail to bind in either direction (panels A and B). Structural alignment of zfAAC$_{60–166}$ and bAAC$_{59–163}$ structures is shown as a stereo pair in panel C. Although the binding directions differ in these two crystal structures, several molecular interactions are conserved. The two hydrophobic residues isoleucine 159 and valine 161 bury into the alpha crystallin core domain. Proline 160 is centrally located on a pseudo twofold axis. Arginines 157 and 163 point in the same direction with similar molecular interactions.

complex (Supporting Information Fig. S3, lane 2) presumably arises from molecular interactions of the C-terminal extension with adjacent zfAAC$_{60–166}$ chains. This observation shows that a small percentage of the C-terminal extensions have entered the 3D domain swapped state by heating AAC at a concentration of 1 mg/mL to 37°C for 1 h followed by rapidly cooling on ice. This result supports a modest energetic barrier to 3D domain swapping. A modest energy barrier would support a dynamic polydisperse oligomeric assembly with the ability of subunits to readily exchange. This is in direct agreement with other experimental work.[30,31]

Discussion

Alpha crystallins are highly dynamic proteins exhibiting structural plasticity.[1,7,14,30–34] Regardless of whether the C-terminal extension in a swapped or closed state, the C-terminal hinge loop maintains structural rigidity while offering enough structural

flexibility to enable various oligomeric interactions. Our observation of both swapped and closed states of the C-terminal extension establish another molecular mechanism by which the alpha crystallins maintain polydisperse oligomeric assemblies. 3D domain swapping, added to bidirectional binding, various AP interface registrations, and a flexible hinge loop of our previous work,[1] show that at least four molecular mechanisms have evolved for the eye lens alpha crystallins to frustrate crystallization and to maintain eye lens function.

Material and Methods

Protein expression and purification

Plasmid construction, protein expression, and purification were performed as previously described.[1] Briefly, zebrafish (*D. rerio*) AAC residues 60–166 was cloned into pET28b (Novagen, Gibbstown, NJ) with tobacco etch virus (TEV) protease cleavable N-terminal His-tag. Proteins were purified by affinity chromatography, followed by TEV protease cleavage of N-terminal His-tag, and final purification by gel filtration chromatography in gel filtration (GF) buffer (20 m*M* TRIS pH 8.0, 100 m*M* sodium chloride, 1 m*M* DTT). Proteins were concentrated and stored at 4°C prior to use. Protein concentration was determined by absorbance at 280 nm with the calculated extinction coefficient of 0.47.

Protein crystallization

Concentrated $zfAAC_{60–166}$ was diluted to 8 mg/mL in GF buffer, and crystals were grown in hanging drop VDX plates (Hampton Research, Aliso Viejo, CA) in condition Qiagen PACT B3 (0.1*M* MIB (2:3:3—sodium malonate:imidazole:boric acid) buffer pH 6.0, 25% PEG 1500) in a ratio of 1:2 of protein:well solution at 20°C. Crystals appeared in 1–3 days of 50–100 μm in size. Crystals were mounted with CrystalCap HT Cryoloops (Hampton Research, Aliso Viejo, CA), and briefly soaked in a cryoprotection solution (0.1*M* MIB buffer pH 6.0, 25% PEG 1500, 20% glycerol) prior to flash freezing in liquid nitrogen. Long soaking times in cryoprotection solution leads to crystal damage and cracking.

Data collection and structure determination

Flash frozen cryoprotected crystals of $zfAAC_{60–166}$ were used for data collection at APS beamline 24-ID-E. Data collection sets were collected at a set distance of 300 mm with a detector 2θ of 0° and 18°. Data were processed using DENZO[35] and SCALEPACK.[35] Phases were obtained by molecular replacement with pdb 3L1E using Phaser[36] and followed by 20 cycles of automated model building in ARP/wARP.[37] Further manual model building was done using COOT.[38] Model refinement was done using PHENIX.[39]

Native polyacrylamide gel electrophoresis

$zfAAC_{60–166}$ stored at 4°C was diluted to 1 mg/mL in GF buffer. The sample was then incubated at 37°C for 1 h, followed by rapidly cooling on ice. The control sample was stored on ice during the 1-h incubation period. The two samples were run on an 8–25% native gel using the pharmacia phast system (GE Healthcare, Piscataway, NJ) according to manufacturer protocol. The resulting native gel was stained with coomassie.

Acknowledgments

The authors thank Duilio Cascio, Joseph Horwitz, Meytal Landau, and Mike Sawaya for useful discussion, Mason Posner for zebrafish alpha crystallin clones, UCLA-DOE X-ray Crystallography Core Facility, Jason Navarro at the UCLA Crystallization Facility, M. Capel, K. Rajashankar, F. Murphy, J. Schuermann, and I. Kourinov at NE-CAT beamline 24-ID-E at APS, and NIH, NSF, and HHMI for support.

References

1. Laganowsky A, Benesch JLP, Landau M, Ding L, Sawaya M, Cascio D, Huang Q, Robinson CV, Horwitz J, Eisenberg D (2010) Crystal structures of truncated alphaA and alphaB crystallins reveal structural mechanisms of polydispersity important for eye lens function. Protein Sci 19:1031–1043.
2. Greiling TM, Houck SA, Clark JI (2009) The zebrafish lens proteome during development and aging. Mol Vis 15:2313–2325.
3. Posner M, Hawke M, Lacava C, Prince CJ, Bellanco NR, Corbin RW (2008) A proteome map of the zebrafish (*Danio rerio*) lens reveals similarities between zebrafish and mammalian crystallin expression. Mol Vis 14: 806–814.
4. de Jong WW. Evolution of lens and crystallins. In: Bloemendal H, Ed. (1981) Molecular and cellular biology of the eye lens. New York: Wiley, pp 221–278.
5. Marvin M, O'Rourke D, Kurihara T, Juliano CE, Harrison KL, Hutson LD (2008) Developmental expression patterns of the zebrafish small heat shock proteins. Dev Dyn 237:454–463.
6. Goishi K, Shimizu A, Najarro G, Watanabe S, Rogers R, Zon LI, Klagsbrun M (2006) AlphaA-crystallin expression prevents gamma-crystallin insolubility and cataract formation in the zebrafish *cloche* mutant lens. Development 133:2585–2593.
7. Bagneris C, Bateman OA, Naylor CE, Cronin N, Boelens WC, Keep NH, Slingsby C (2009) Crystal structures of alpha-crystallin domain dimers of alphaB-crystallin and Hsp20. J Mol Biol 392:1242–1252.
8. Jehle S, van Rossum B, Stout JR, Noguchi SM, Falber K, Rehbein K, Oschkinat H, Klevit RE, Rajagopal P (2009) AlphaB-crystallin: a hybrid solid-state/solution-state NMR investigation reveals structural aspects of the heterogeneous oligomer. J Mol Biol 385:1481–1497.
9. Berengian AR, Bova MP, McHaourab HS (1997) Structure and function of the conserved domain in alphaA-crystallin. Site-directed spin labeling identifies a beta-strand located near a subunit interface. Biochemistry 36:9951–9957.
10. Berengian AR, Parfenova M, McHaourab HS (1999) Site-directed spin labeling study of subunit interactions in

the alpha-crystallin domain of small heat-shock proteins. Comparison of the oligomer symmetry in alphaA-crystallin, HSP 27, and HSP 16.3. J Biol Chem 274:6305–6314.
11. Koteiche HA, Berengian AR, McHaourab HS (1998) Identification of protein folding patterns using site-directed spin labeling. Structural characterization of a beta-sheet and putative substrate binding regions in the conserved domain of alpha A-crystallin. Biochemistry 37:12681–12688.
12. Benedek G (1983) Why the eye lens is transparent. Nature 302:383–384.
13. Benedek GB (1971) Theory of transparency of the eye. Appl Opt 10:459–473.
14. Delaye M, Tardieu A (1983) Short-range order of crystallin proteins accounts for eye lens transparency. Nature 302:415–417.
15. Veretout F, Delaye M, Tardieu A (1989) Molecular basis of eye lens transparency. Osmotic pressure and X-ray analysis of alpha-crystallin solutions. J Mol Biol 205: 713–728.
16. Gronenborn AM (2009) Protein acrobatics in pairs—dimerization via domain swapping. Curr Opin Struct Biol 19:39–49.
17. Carey J, Lindman S, Bauer M, Linse S (2007) Protein reconstitution and three-dimensional domain swapping: benefits and constraints of covalency. Protein Sci 16: 2317–2333.
18. Bennett MJ, Sawaya MR, Eisenberg D (2006) Deposition diseases and 3D domain swapping. Structure 14: 811–824.
19. Liu Y, Eisenberg D (2002) 3D domain swapping: as domains continue to swap. Protein Sci 11:1285–1299.
20. Rousseau F, Schymkowitz JW, Itzhaki LS (2003) The unfolding story of three-dimensional domain swapping. Structure 11:243–251.
21. van Montfort RL, Basha E, Friedrich KL, Slingsby C, Vierling E (2001) Crystal structure and assembly of a eukaryotic small heat shock protein. Nat Struct Biol 8: 1025–1030.
22. Kim KK, Kim R, Kim SH (1998) Crystal structure of a small heat-shock protein. Nature 394:595–599.
23. Bloemendal H, de Jong W, Jaenicke R, Lubsen NH, Slingsby C, Tardieu A (2004) Ageing and vision: structure, stability and function of lens crystallins. Prog Biophys Mol Biol 86:407–485.
24. Blundell T, Lindley P, Miller L, Moss D, Slingsby C, Tickle I, Turnell B, Wistow G (1981) The molecular structure and stability of the eye lens: X-ray analysis of gamma-crystallin II. Nature 289:771–777.
25. Bax B, Lapatto R, Nalini V, Driessen H, Lindley PF, Mahadevan D, Blundell TL, Slingsby C (1990) X-ray analysis of beta B2-crystallin and evolution of oligomeric lens proteins. Nature 347:776–780.
26. Smith MA, Bateman OA, Jaenicke R, Slingsby C (2007) Mutation of interfaces in domain-swapped human beta B2-crystallin. Protein Sci 16:615–625.
27. Van Montfort RL, Bateman OA, Lubsen NH, Slingsby C (2003) Crystal structure of truncated human beta B1-crystallin. Protein Sci 12:2606–2612.
28. Aravind P, Suman SK, Mishra A, Sharma Y, Sankaranarayanan R (2009) Three-dimensional domain swapping in nitrollin, a single-domain betagamma-crystallin from *Nitrosospira multiformis*, controls protein conformation and stability but not dimerization. J Mol Biol 385:163–177.
29. Bennett MJ, Choe S, Eisenberg D (1994) Domain swapping: entangling alliances between proteins. Proc Natl Acad Sci USA 91:3127–3131.
30. Aquilina JA, Benesch JL, Bateman OA, Slingsby C, Robinson CV (2003) Polydispersity of a mammalian chaperone: mass spectrometry reveals the population of oligomers in alphaB-crystallin. Proc Natl Acad Sci USA 100:10611–10616.
31. Aquilina JA, Benesch JL, Ding LL, Yaron O, Horwitz J, Robinson CV (2005) Subunit exchange of polydisperse proteins: mass spectrometry reveals consequences of alphaA-crystallin truncation. J Biol Chem 280: 14485–14491.
32. Benesch JL, Ayoub M, Robinson CV, Aquilina JA (2008) Small heat shock protein activity is regulated by variable oligomeric substructure. J Biol Chem 283: 28513–28517.
33. Bova MP, Ding LL, Horwitz J, Fung BK (1997) Subunit exchange of alphaA-crystallin. J Biol Chem 272: 29511–29517.
34. Horwitz J (1992) Alpha-crystallin can function as a molecular chaperone. Proc Natl Acad Sci USA 89:10449–10453.
35. Otwinowski Z, Minor W (1997) Processing of X-ray diffraction data collected in oscillation mode. Methods Enzymol 276:307–326.
36. McCoy AJ, Grosse-Kunstleve RW, Adams PD, Winn MD, Storoni LC, Read RJ (2007) Phaser crystallographic software. J Appl Crystallogr 40:658–674.
37. Langer G, Cohen SX, Lamzin VS, Perrakis A (2008) Automated macromolecular model building for X-ray crystallography using ARP/wARP version 7. Nat Protoc 3:1171–1179.
38. Emsley P, Cowtan K (2004) Coot: model-building tools for molecular graphics. Acta Crystallogr D Biol Crystallogr 60:2126–2132.
39. Adams PD, Grosse-Kunstleve RW, Hung LW, Ioerger TR, McCoy AJ, Moriarty NW, Read RJ, Sacchettini JC, Sauter NK, Terwilliger TC (2002) PHENIX: building new software for automated crystallographic structure determination. Acta Crystallogr D Biol Crystallogr 58: 1948–1954.